

MECHANICAL CHARACTERIZATION OF PARTICLE-INFUSED ELASTOMERIC SYSTEMS

Comtois-Arnaldo, C and Petel, OE*

Mechanical and Aerospace Engineering, Carleton University, Ottawa, ON, Canada

* Corresponding author (oren.petel@carleton.ca)

Keywords: *particulate system, mechanical characterization, strain rate sensitivity*

ABSTRACT

In the present study, the mechanical properties of particle-reinforced polymer composites are investigated. The mechanical behaviour exhibited by these particulate systems is shown to vary substantially with loading rate due to the effects of particle interactions. The response of these multiphase systems is investigated through a siloxane elastomer that has been doped with micron-sized ceramic particles (aluminum oxide and silicon carbide), at various volume fractions. This investigation focuses on the mechanical characterization of the particulate systems under tension and shear loading at quasi-static strain rates. Mechanical properties are extracted from stress-strain data collected using an MTS machine in order to identify relevant trends as the strain rate is increased. Results demonstrate that the filler particle type influences the overall material properties.

1 INTRODUCTION

Particle-laden polymer composite systems are a low production cost class of materials that provides a degree of control over their mechanical properties through microstructure variations. As a result, these materials have found widespread industrial uses in military, automotive, food packaging, dentistry, and tissue engineering applications [1-5]. The introduction of hard ceramic inclusions to polymeric or metal matrices has been previously studied [5-8], resulting in a general consensus that bulk material strength and stiffness increases with an increase in both filler quantity and loading rate. Other studies have claimed the exact opposite effect [8,9].

Polymer-particulate systems require extensive characterization due to their high sensitivity to strain rate variations. It is therefore important to characterize these material systems under the anticipated loading scenario in order to properly design for a specific application. Arias et al. [5] calculated the static compressive properties of an alumina-polymer composite at various volume fractions by using the individual component properties within the system. Applying a uniform-stress hypothesis yielded an inverse rule of mixtures that accurately models the response of the system when compared to experimental data. Werner et al. [10] developed a general three-dimensional elastic-viscoplastic constitutive model for an epoxy matrix using a series of uniaxial tests (i.e., tension, compression, and shear) at several strain rates; however, the accuracy involving an extrapolation beyond the validation range remains questionable.

The polymer matrix of a particulate composite loaded at a quasi-static rate should be expected to have a significant effect on the composite behaviour. In the case of extreme strain rates, such as those approaching the ballistic range, the polymeric matrix has a diminished influence on the overall dynamic response of the composite. A similar behaviour was observed in dense particle suspensions, where the relative compressibility between the inclusion and matrix phases leads to a local increase in apparent particle volume fraction [11,12]. This compressibility effect makes particle-particle interactions more prominent and an exceedingly dominant factor in the material behaviour at extreme strain rates, and particularly important in ballistic events [13,14]. A split Hopkinson pressure bar study by Jordan et al. [9] supports the latter statement, showing that at a particle volume fraction approaching 50%, the compressive

strength of a polymer composite is independent of the polymer matrix and becomes dominated by the particle-particle interactions.

The present study investigates the quasi-static tensile and shear strength of a siloxane elastomer doped with various ceramic particles at two strain rates in order to identify the effect of hard inclusions in an elastomeric matrix. The study focuses on variations in particle material as well as the loading fraction of the particles within the matrix. Results from this study will provide alternative parametric variation for this class of material in an effort to improve empirical polymer composite model development.

2 MATERIAL DESCRIPTION AND SAMPLE PREPARATION

2.1 *Multiphase particulate system*

The composite under investigation in the present study was a two-phase system consisting of an elastomeric matrix embedded with micron-sized ceramic particles. An elastomer is an amorphous polymer whose flexible chains are cross-linked together by covalent bonds, resulting in an extremely high extensibility and exhibits complete recovery after deformation [15,16]. The polymer matrix chosen for this study was a polydimethylsiloxane (PDMS) elastomer, Sylgard 184 (Dow Corning), commonly used for microfluidic applications [17]. Sylgard 184 is supplied as a two-part liquid component kit: a pre-polymer base and a curing agent having a recommended mix ratio of 10:1 (by weight). The ceramic filler material consisted of a 1000-grit fused alumina (Al_2O_3) powder, supplied by Panadyne. The alumina powder had an irregular/blocky morphology as seen in Figure 1. A 600-grit silicon carbide (SiC) powder with similar morphology, supplied by Panadyne, was used as the second filler material for comparison purposes. The particle size distribution of both powders, as supplied by the manufacturer, can be found in Table 1. For the present study, silicon carbide particles were integrated into the PDMS matrix at 4.7%, 23.6%, and 33.3% volume fraction while alumina-PDMS composites were prepared at a single volume fraction: 33.3%.

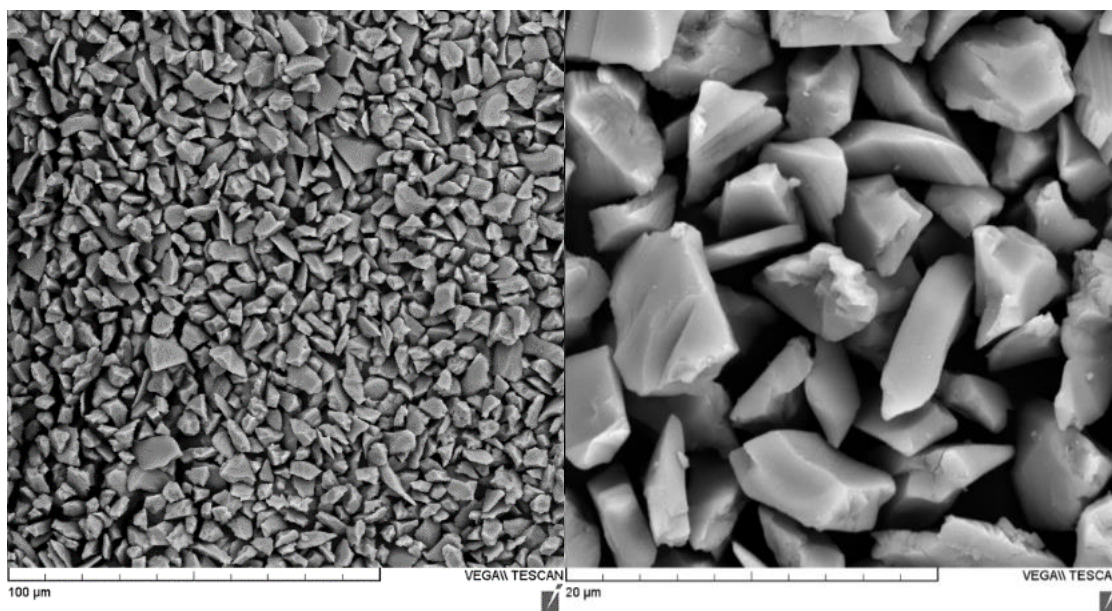


Figure 1. SEM images of the 1000-grit fused alumina particles

Particle Type	Particle Size (microns)			Chemistry (%)						
	D3%	D50%	D94%	Al ₂ O ₃	SiC	Fe ₂ O ₃	Na ₂ O	SiO ₂	Si	C
1000-grit Al ₂ O ₃	6.95	4.35	2.98	99.30	-	0.08	0.45	0.08	-	-
600-grit SiC	16.63	9.01	4.3	-	99.11	0.09	-	0.16	0.11	0.16

Table 1. Certificate of analysis results provided by the supplier (Panadyne)

2.2 Sample production methodology

Tensile dumbbells and shear puck specimens were prepared through a low-cost cast moulding process and cured at room temperature for 48 hours prior to removal. Moulds were designed according to their respective American Standard Test Method (ASTM) specifications [18,19] and were 3D-printed from ABSplus-P430 using an in-house Dimension SST 1200es. The polymer composite manufacturing procedure is described below:

- 1) Integration of particles into the pre-polymer base liquid through thorough mechanical mixing
- 2) Heating of base-particulate mixture in conventional oven at approximately 100°C for 10 minutes to decrease viscosity prior to ultrasonication since alumina particles dramatically thicken the liquid
- 3) Ultrasonication of the mixture in a water bath for 30-45 minutes in order to break up aggregations and obtain a homogeneous distribution of particles within the base liquid
- 4) Once the mixture has returned to room temperature, introduce curing agent to the solution at a 10:1 base-curing agent mix ratio, as per manufacturer recommendations [20], followed by thorough mechanical mixing
- 5) Desiccation of solution for approximately 1.5 hours to remove trapped air
- 6) Transfer mixture to the moulds and remove resulting trapped air near the surface
- 7) Set moulds onto flat surface and allow to cure under atmospheric conditions

Tension moulds have been lightly coated with a polyester mould-release spray prior to the transfer of the elastomer solution (step 6) since the cured material tends to snag and tear at the neck transition regions upon removal from the mould, providing a strain concentration that resulted in premature sample failure upon testing. This process minimized sample removal damage, demonstrating the sensitivity of elastomer systems to the presence of small defects.

3 MECHANICAL CHARACTERIZATION

Quasi-static investigations of the behaviour of a particulate composite and its baseline elastomer matrix were performed through the use of hydraulic MTS machines. Stress-strain curves of the materials were measured under tensile and shear loading scenarios at two strain rates, allowing a limited discussion of loading rate sensitivity for the materials.

3.1 Shear testing

Shear strength experiments were conducted with a shear punch tool (Figure 2) manufactured according to specifications described in ASTM D732-10 [18]. Six disk-shaped specimens with a 50 mm diameter and approximately 6.35 mm thickness were prepared for each testing scenario. Sample thicknesses were calculated by measuring each disk quadrant with calipers and averaging the results.



Figure 2: Shear punch tool (ASTM D732) and setup

The MTS hydraulic press was configured to travel at constant displacement rates, either 1.3 mm/min (slow) or 3000 mm/min (fast). The press forced the punch through the test material and extracted a shear plug from the test specimen. Figure 3 displays typical shear stress curves for neat Sylgard 184 as well as for composites loaded with either alumina or silicon carbide at the stated volume fractions and displacement rate. Normalized displacement is defined as the distance that the punch travels within the sample relative to its thickness and is not necessarily representative of the strain experienced by the specimen. Through experimental observations, it was confirmed that the point of maximum shear stress represents the onset of shear failure at the top surface of the specimens; the remaining portion of the curves passed the point of failure has been omitted for clarity purposes.

It can be seen that the alumina-PDMS composite exhibits a significantly different response as compared to the SiC-PDMS specimen of equivalent volume fraction in terms of both higher strength and stiffness. These results clearly demonstrate that the quasi-static shear strength of an elastomeric composite increases with volume fraction but is also strongly dependent on particle type.

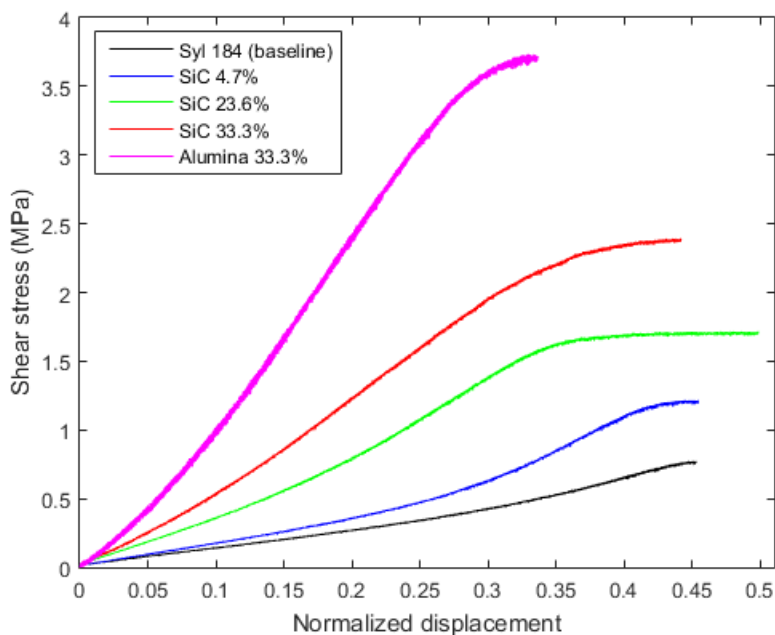


Figure 3. Shear stress curves for baseline and various composites (1.3 mm/min rate)

Some inconsistencies in shear data were found when reversing the specimen loading orientation as compared to the cure orientation of the sample, i.e., switching the surface in contact with the shear punch (Figure 4). Results suggest that particle settling during the long cure process may have influenced the peak shear stress measurement, however this could be avoided by reducing cure times through the use of an oven. Distinctive features within the shear curves arise depending on whether the punch makes contact with the top surface of the cured specimen first (TSF) or the bottom surface first (BSF). These acronyms will be employed from now on to distinguish between the two different loading orientations. It should be noted that the results for a given orientation were highly reproducible, based on repeated experimentation.

The effect of strain rate on the baseline system and the 33.3% alumina-PDMS composite is presented in Figure 4. A typical curve for both orientations of alumina samples is displayed; pure elastomer specimens show no sensitivity to loading orientation due to the absence of particles within the system. The solid lines found in Figure 4 represent the slower strain rate test (1.3 mm/min) while the dotted lines consist of the data from the relatively faster displacement rate trials (3000 mm/min). Unlike in Figure 3, the entire shear curves are displayed in order to see the total effect of strain rate. It should be noted that the specimen orientation is an especially important factor at slow strain rates as seen by the varying shear strengths, however, as the strain rate increases, specimen orientation becomes less significant and shear strengths converge to a single value.

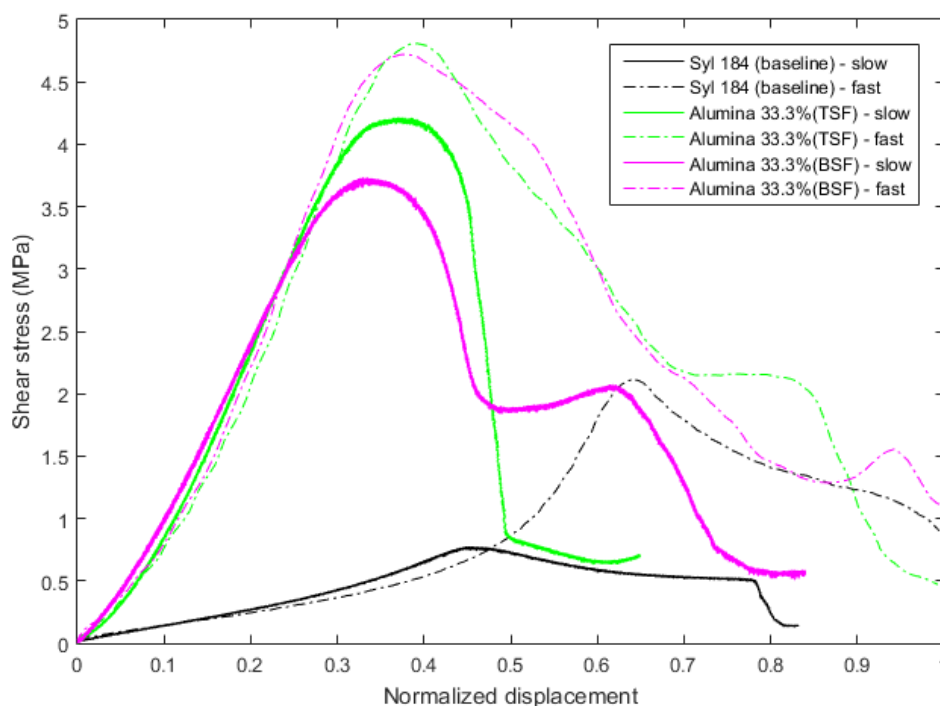


Figure 4. Effect of strain rate on shear stress curves for baseline elastomer and alumina-PDMS composites

3.2 Tensile testing

Tensile stress data were obtained in accordance with the standards described in ASTM D412-06a [19]. Dumbbell specimens having a type C geometry were prepared according to the procedure described in section 2.2. The test section thickness for each sample was measured with a micrometer, while taking care to not compress the highly

MECHANICAL CHARACTERIZATION OF PARTICLE-INFUSED ELASTOMERIC SYSTEMS

elastic material, and subsequently averaged for each sample. Specimen widths were measured using a shadowgraph: a non-intrusive measuring technique which allows the user to extract geometrical dimensions without physically interacting with the material and potentially deforming it. Support tabs were added to both sides of the dumbbell extremities using double-sided adhesive tape so that the MTS machine jaws provide a uniform pressure distribution without damaging the sample when securing the ends prior to testing. The gauge length used to calculate engineering strain was measured as the distance between these support tabs.

Tensile stress-strain data for the baseline elastomer as well as the alumina-PDMS composite are shown below. Two elongation rates were specified for tensile testing: 0.5 mm/s (slow) and 100 mm/s (fast). Both curves are shown for the alumina-PDMS composite, however, only the slow rate data is plotted for the baseline elastomer.

It should be noted that the data presented in Figure 5 were obtained directly from the MTS software. For specimens experiencing large strain values, such as elastomers, it is important to recognize that the shouldered sections of the dumbbell geometry contribute to the overall strain experienced by the system [22] and not only the test section, thus, overestimating the actual strain of the test section. Schneider et al. computed a correction factor of $m = 0.50$ to scale the strain values in the quasi-linear stress-strain regime (up to 40% strain) and account for this overcompensation. No correction factor has yet to be applied to the present data.

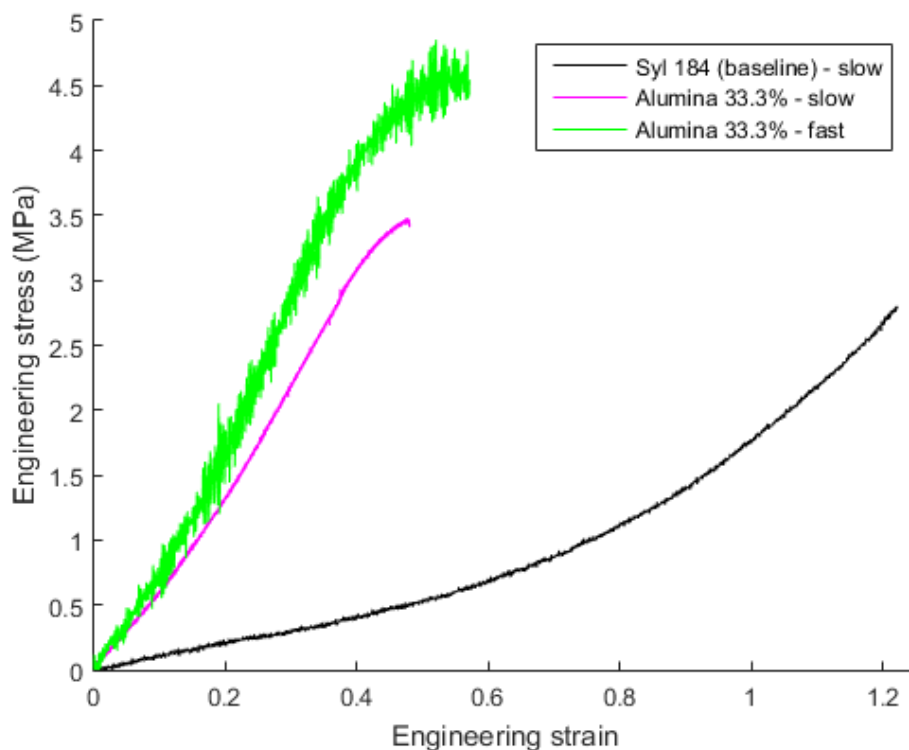


Figure 5. Tensile stress-strain curves for elastomer and alumina-PDMS composite at two elongation rates

4 DISCUSSION

Several particle-elastomer composite systems were tested under shear and tensile loading at different strain rates, demonstrating some interesting results that require further consideration. The shear results obtained in the present study illustrated that increasing the SiC volume fraction within the PDMS matrix also increases the composite stiffness and shear strength (Figure 3), which was to be expected. Figure 3 also shows differences in both composite stiffness and strength between specimens containing SiC or alumina particles at equivalent volume fractions. The difference measured in the response of these two material systems was not expected to be so large, based on typical mixture models. Mechanical properties for the filler particles and matrix under investigation are given in Table 2. If we use either mass fraction or volume fraction-based mixture models, the small differences in particle stiffness and densities cannot account for the 75% increase in stiffness observed for alumina-PDMS specimens over their SiC counterparts under shear loading. Although SiC has higher stiffness and hardness, alumina is approximately 23% denser. This should not have had such a dramatic effect in the quasi-static range. It should be noted that the alumina particles are approximately half the characteristic length of the SiC particles (Table 1), which could be a factor justifying the increased strength. Another possible explanation of the results is an effect relating to the particle-matrix interface adhesion based on the wetted areas and particle morphology, although this has not been quantified.

Material	Density (g/cc)	Poisson's Ratio	Young's Modulus (GPa)	Hardness (Mohs)	Compressive Strength (MPa)
Sylgard 184	1.03	0.45-0.5	$1.32-1.8 \times 10^{-3}$	-	-
Al ₂ O ₃	3.95-3.99	0.21-0.27	344.7-408.9	9.0	2944.1
SiC	3.21	0.183-0.192	410.2-440.6	9.2	565.4-1379.0

Table 2. General mechanical properties of ceramics under investigation [20,22-26]

The effect of strain rate on the shear stress curves of the baseline elastomer and alumina-PDMS specimens showed some interesting trends worth consideration (Figure 4). When comparing the two curves for the baseline elastomer, it appears that its shear strength is significantly higher at elevated strain rates, increasing by over 100%. It is also worth noting that the onset of shear failure was also delayed to higher strain levels with increasing strain rates. Alternatively, the shear strength for the alumina-PDMS composite is much less sensitive to strain rates and has increased by 23%, although the baseline low strain rate shear strength is dramatically higher than that of the matrix PDMS itself. The apparent stiffness in the quasi-linear region of the curves has remained constant for both particulate specimens, regardless of strain rate, suggesting that particle-particle interactions are not particularly important at these strain rates. The material behaviour is therefore primarily dominated by the strain sensitivity of the matrix itself.

When loading the alumina-PDMS composite at the low strain rate, it was found that once the material reached its peak shear stress, it would suddenly undergo tensile failure due to bending stress and subsequent crack propagation within the matrix, resulting in the sudden loss of strength seen in Figure 4. At higher strain rates, the behaviour appears to be primarily dominated by shear failure. This appears to be a purely rate-dependent failure response, which is characterized by a more shallow slope of the shear stress at increasing shear punch displacement, once the shear strength has been exceeded.

The tensile strength data obtained for Sylgard 184 (Figure 5) fluctuated significantly due to its low fracture toughness, resulting in sudden failure in the presence of any small defect within the specimens. This effect is likely responsible

for the variability in published data for this material [20,22], which varied slightly from our own measurements. Although there was evidence of voids on the fracture surfaces of the alumina-PDMS specimens when loaded at the low strain rate, the stress-strain curve trends were extremely reproducible. It is assumed that the fracture toughness measured for these specimens was influenced by a slightly premature failure, although this influence was more significant in the PDMS testing. Removing all porosity in high concentration particulate composites is extremely complicated and requires further refinement of the manufacturing technique to ensure adequate accuracy in our fracture toughness measurement.

For the tensile loading, an increase in the strain rate resulted in an increase of the elastic modulus and tensile strength of the alumina-PDMS specimens, as seen in Figure 5. Interestingly, no obvious voids were present on the fracture surface of these alumina-PDMS specimens loaded at the higher strain rates, so the fracture toughness may be more accurate at these strain rates. Evidence of plastic deformation was noticed in the alumina-PDMS composite curves prior to failure, thus, showing signs of improved fracture toughness. While this could be a strain rate effect it could also be the result of a seemingly reduced influence of internal porosity on the failure event.

5 CONCLUSION

Ceramic particles have been integrated into an elastomeric matrix at various volume fractions and characterized through tensile and shear loading at two strain rates. The following conclusions can be made from this study:

- As particle volume fraction is increased, the shear strength and stiffness of the composite increased as well. The resulting strength and stiffness of the polymer composite is strongly dependent on the particle type, which may be the result of surface chemistry influencing the distribution of the filler phase within the matrix.
- The shear strength of the PDMS matrix is strongly dependent on strain rate.
- The stiffness of the elastomer and alumina-PDMS specimens under shear loading do not appear to be rate dependent. This suggests that particle-particle interactions are likely not particularly relevant to the material response at these strain rates.
- Sample orientation variations under shear loading demonstrate that the curing process was not optimized and should be altered to minimize particle settling. The effect of particle settling on the response of the materials was diminished at increasing loading rates.
- The dominant failure mechanism in the shear loaded alumina-PDMS specimens was influenced by the loading rate.
- The tensile strength and elastic modulus of the alumina-PDMS composite increased with loading rate.

6 REFERENCES

- [1] A. Okada, and A. Usuki. "Twenty-Year Review of Polymer-Clay Nanocomposites at Toyota Central R&D Labs., Inc.". SAE Technical Paper 2007-01-1017, DOI: 10.4271/2007-01-1017, 2007.
- [2] T.V. Duncan. "Applications of nanotechnology in food packaging and food safety: barrier materials, antimicrobials and sensors". Packing World. Available: <https://www.packworld.com/sustainability/strategy/nanotechnology-packs-promise> [Feb 7, 2017].
- [3] S.B. Mitra, D. Wu, and B.N. Holmes. "An application of nanotechnology in advanced dental materials". *Journal of the American Dental Association*. Vol. 134, pp 1382-1390, 2003.
- [4] I. Armentano, M. Dottori, E. Fortunati, S. Mattioli, and J.M. Kenny. "Biodegradable polymer matrix nanocomposites for tissue engineering: a review". *Journal of Polymer Degradation and Stability*, 95, pp 2126-2146, 2010.

MECHANICAL CHARACTERIZATION OF PARTICLE-INFUSED ELASTOMERIC SYSTEMS

- [5] A. Arias, R. Zaera, J. López-Puente, C. Navarro. “Numerical modeling of the impact behavior of new particulate-loaded composite materials”. *Journal of Composite Structures*, 61, pp 151-159, 2003.
- [6] Y. Li and K.T. Ramesh. “Influence of particle volume fraction, shape, and aspect ratio on the behavior of particle-reinforced metal-matrix composites at high rates of strain”. *Acta mater*, Vol. 46, pp5633-5646, 1998.
- [7] P. Moy, T. Weerasooriya, and W. Chen. “Mechanical response of polycarbonate nano-composites as a function of strain rate and weight percent of nano-silicate clay loading”. *Proceedings of the 2012 Annual Conference on Experimental and Applied Mechanics*, Vol. 1, ch. 3, pp 17-20, 2013.
- [8] A.S. Jones. “Low strain rate studies of alumina-epoxy composites using piezospectroscopy”. M.S. thesis, Dept. of Mech. and Aero. Engineering, Orlando, Florida, 2013.
- [9] J.L. Jordan and J.E. Spowart. “Comparison of mechanical properties of polymer-based multi-phase particulate composites”. *Journal of Dynamic Behavior of Materials*, Vol. 1, pp 317-320, 2013.
- [10] B.T. Werner and I.M. Daniel. “Characterization and modeling of polymeric matrix under static and dynamic loading”. *Proceedings of the 2012 Annual Conference on Experimental and Applied Mechanics*, Vol. 1, ch. 10, pp 73-84, 2013.
- [11] O.E. Petel and A.J. Higgins. “Shock wave propagation in dense particle suspensions”. *Journal of Applied Physics*, 108(11), 114918, 2010.
- [12] O. E. Petel, D.L. Frost, A.J. Higgins, and S. Ouellet. “Formation of a disordered solid via a shock-induced transition in a dense particle suspension”. *Physical Review E*, 85(2), 021401, 2012.
- [13] O. E. Petel, S. Ouellet, J. Loiseau, B.J. Marr, D.L. Frost, and A.J. Higgins. “The effect of particle strength on the ballistic resistance of shear thickening fluids”. *Applied Physics Letters*, 102(6), 064103, 2013.
- [14] O.E. Petel, S. Ouellet, J. Loiseau, D.L. Frost, and A.J. Higgins. « A comparison of the ballistic performance of shear thickening fluids based on particle strength and volume fraction”. *International Journal of Impact Engineering*, 85, pp 83-96, 2015.
- [15] N.G. McCrum, C.P. Buckley, C.B. Bucknall. “The Elastic Properties of Rubber” in *Principles of Polymer Engineering*, 2nd ed., ch.3, New York, Oxford University Press Inc., 1997.
- [16] J. Karger-Kocsis, S. Fakirov. “Rubber Nanocomposites: New Developments, New Opportunities” in *Nano-and Micro-Mechanics of Polymer Blends and Composites*, ch.4, Munich, Germany, Hanser, 2009.
- [17] J. Friend and L. Yeo. “Fabrication of microfluidic devices using polydimethylsiloxane”. *Journal of Biomicrofluidics*, Vol. 4, 026502, 2010.
- [18] ASTM Standard D732, 2010, “Shear strength of plastics by punch tool”. ASTM International, West Conshohocken, PA, 1943, DOI: 10.1520/D0732-10, www.astm.org.
- [19] ASTM Standard D412, 2013, “Vulcanized rubber and thermoplastic elastomers – tension”. ASTM International, West Conshohocken, PA, 1935, DOI: 10.1520/D0412-06AR13, www.astm.org.
- [20] Dow Corning. “Product information Sylgard® 184 silicone elastomer”. Available: <http://www.dowcorning.com/Applications/search/default.aspx?R=131EN> [Sept 15, 2015].
- [21] J. Blaber and A. Antoniou. “Ncorr – Instruction manual”. Georgia Institute of Technology, Version 1.2.1, 2015.
- [22] F. Schneider, T. Fellner, J. Wilde, and U. Wallrabe. “Mechanical properties of silicones for MEMS”. *Journal of Micromechanics and Microengineering*, 18, 065008, 2008.
- [23] J.E. Mark. “*Polymer Data Handbook*”. New York: Oxford University Press, 1999.
- [24] V. Struder *et al.* “Scaling properties of a low-actuation pressure microfluidic valve”. *Journal of Applied Physics*, 95 393-8, 2004.
- [25] J.F. Shackelford and W. Alexander. “*Material science and engineering handbook*”. 3rd ed., CRC Press, 2001.
- [26] I.D. Johnston *et al.* “Mechanical characterization of bulk Sylgard 184 for microfluidics and microengineering”. *Journal of Micromechanics and Microengineering*, 24, 035017, pp 1-7, 2014.